Cement and Concrete Research 41 (2011) 496–503

Contents lists available at ScienceDirect

Cement and Concrete Research

journal homepage: http://ees.elsevier.com/CEMCON/default.asp

Flow of fresh concrete through steel bars: A porous medium analogy

K. Vasilic [a], B. Meng [a], H.C. Kühne [a], N. Roussel [b,*]

[a] BAM, Federal Institute for Materials Research and Testing, Berlin, Germany
[b] Université Paris Est, Laboratoire Central des Ponts et Chaussées, Département Matériaux, Paris, France

ARTICLE INFO

Article history:
Received 10 May 2010
Accepted 19 January 2011

Keywords:
Fresh concrete (A)
Rheology (A)
Modeling (E)
Permeability(C)
Yield stress

ABSTRACT

Although being a very promising area of concrete technology, computational modeling of fresh concrete flow is a comprehensive and time consuming task. The complexity and required computation time are additionally increased when simulating casting of heavily reinforced sections, where each single reinforcement bar has to be modeled. In order to improve the computation speed and to get closer to a practical tool for simulation of casting processes, an innovative approach to model reinforced sections is proposed here. The basic idea of this approach is to treat the reinforcement zone as a porous medium in which a concrete is propagating. In the present paper, the numerical implementation of this concept is described. A methodology allowing for the computation of the equivalent permeability of the steel bars network is suggested. Finally, this numerical technique efficiency is evaluated by a comparison with experimental results of model fluids casting in model formworks.

1. Introduction

During the last decade, numerical modeling of fresh concrete flow has become an important tool for the prediction and optimization of casting processes [1–7]. The modeling of the complex rheological behavior of concrete in the fresh state is not a trivial task and the research community still works on development of appropriate rheological and numerical approaches to simulate fresh concrete flow [1,8–16]. In addition to this complex rheological behavior, the influence of reinforcement on the flow has to be taken into account as well. Modeling of each steel bar significantly increases not only computing but also pre-processing time (time for geometry generation and meshing). In order to simplify pre-processing and to reduce computational time, the idea of treating reinforcement as a porous medium was proposed [17–19]. In this approach, the network of steel bars is considered as a homogeneous porous zone (Cf. Fig. 1).

The duration of numerical casting process prediction can be divided in two parts: the pre-processing time during which the geometry and the mesh are generated and computation time during which the fluid mechanics equations are numerically solved at each point of the mesh. It can be seen in the example shown in Fig. 1 that the geometry to be modeled is obviously far simpler in the case of the porous medium analogy. As a consequence, the time needed to generate it will be strongly reduced. It can be moreover expected that, as the number of mesh points decreases, the computation time will also be reduced.

As a first approximation, it is possible to estimate the reduction in pre-processing time and calculation time by considering the following orders of magnitude in ideal computation conditions. In most concrete casting situations, the characteristic size of the flow is of the order of a few tens of cm. This is for example the typical thickness of a wall or a slab. This shall also be the characteristic dimension of the porous medium. When considering steel bars, the characteristic size of the flow is reduced to a few centimeters (*i.e.* 10 times lower). The number of cells to be implemented within the considered characteristic distance is imposed by the numerical convergence criteria. As steel bars are mainly cylindrical obstacles (*i.e.* 2D obstacles), this means that the number of cells will decrease by a factor 100 between the cases with and without steel bars. It can therefore be roughly estimated that the computation time will also decrease by a factor 100. It is more delicate to estimate how the time needed for geometry and mesh generation shall be affected. However, as we are considering here some periodic systems, it is possible to assume that the preprocessing time shall decrease by a factor 10 between the cases with and without steel bars (*i.e.* 10 being the number of obstacles in one direction, the use of copy–paste functions will allow for a fast meshing of the rest of the domain).

Consequently, we suggest here to model the flow of concrete through a reinforced zone as the free surface flow of a yield stress fluid through a continuous porous medium. In the present paper, numerical implementation of this concept is described. A methodology allowing for the computation of the equivalent permeability of the steel bars network is suggested. Finally, this numerical technique efficiency is evaluated through a comparison of numerical predictions with experimental results of model fluids castings in model formworks.

* Corresponding author.
E-mail address: Nicolas.roussel@lcpc.fr (N. Roussel).

0008-8846/$ – see front matter © 2011 Elsevier Ltd. All rights reserved.
doi:10.1016/j.cemconres.2011.01.013

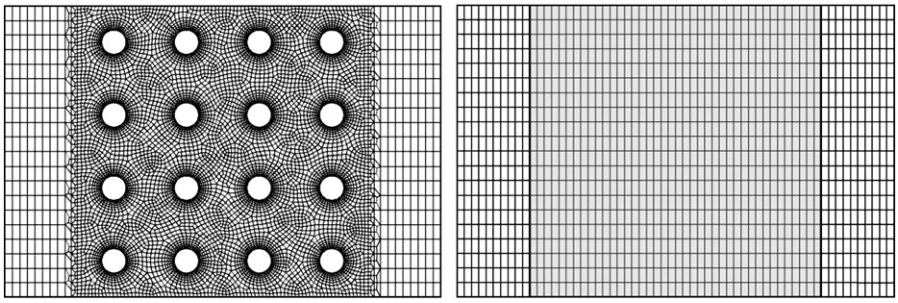

Fig. 1. Schematic representation of steel bars reinforcement (left) treated as a porous medium (right).

2. Porous medium analogy

This section presents the numerical implementation of the porous medium analogy into a general Computational Fluid Dynamics (CFD) software FLUENT©.

2.1. Concrete rheological behavior

From a physical and modeling point of view, fresh concrete can be considered as a fluid (*i.e.* its behavior law shall not depend on the local pressure but only on the local strain rates) when the granular nature of the material can be neglected compared to the hydrodynamic interactions within the material [16,20]. This assumption is fulfilled for stable materials with lower than average contents of coarse aggregates such as concretes with slumps higher than 15 cm and Self Compacting Concrete (SCC) [21,22].

Moreover, identifying concrete as a homogeneous fluid means that, in any two parts of the observed volume, we should find similar ensemble of components [23]. If a physical quantity q (for instance: velocity) is studied, the minimum scale on which one can reasonably observe the system and effectively consider it as a homogeneous fluid thus corresponds to the point beyond which the average of q no longer varies when this scale further increases. The scale of observation is thus of great importance to choose whether or not a homogeneous fluid approach is legitimate. As stated above, the order of magnitude of a formwork smallest characteristic size is of the order of a few tens of cm while the order of magnitude of the size of the coarsest particles is of the order of a couple cm. This means that, if, as a first approximation, the presence of the steel bars is neglected, the flow in a typical formwork can be considered as the flow of a homogeneous fluid.

When steel bars are considered, two things may prevent the use of the above simplifying assumption. First, steel bars may be so close that the gap between two bars is too small to consider that the concrete flow between the bars is homogeneous. We consider here what is called dense reinforcement (*i.e.* 250 kg/m^3) and we consider that bars are parallel cylinders of typical diameter 1 cm (the smaller the diameter, the smaller the gap). The average gap is therefore around 4 cm and it seems therefore possible to consider a homogeneous fluid between these bars as long as particles not larger than roughly 1 cm are used.

Second, blocking of coarse particles may occur between steel bars, leading to non-homogeneities within the material. In [24], a so-called blocking probabilistic parameter P depending on volume of concrete, aggregate volume fraction, maximum diameter and shape of coarse aggregate and gap between the bars was proposed. This parameter captured the transition between blocking and passing. Accordingly, for each particular filling case the corresponding parameter P should be calculated and used as a limiting criteria determining whether yield stress or blocking dominates the flow. If the gaps between the bars are not much larger than the size of coarsest particles it is most probably that the blocking occurs and this limits the proper form filling. If the bar distance is increased and the blocking parameter is higher than the critical value, no blocking occurs and yield stress is the limiting factor for the form filling. In this paper however, we are strictly restricted to the cases where the probability that some of the coarsest aggregates form granular arches within the flow is neglectable [25–27] and we assume that yield stress determines the flow behavior through the obstacles.

Most fluid concretes in standard industrial casting satisfy the above-mentioned constraints and can therefore be described as homogeneous non-Newtonian fluids. The most common constitutive equation used in literature is derived from the Bingham model in its tensorial form and writes:

$$\eta(D_{II}) = \left(\frac{\tau_0}{\sqrt{2D_{II}}} + \eta_{pl}\right) \tag{1}$$

where η is the apparent bulk viscosity, D_{II} is the second invariant of the strain rate tensor (it reduces to the shear rate $\dot{\gamma}$ in 2D simple shear flow problems), τ_0 and η_{pl} are respectively the yield stress and the plastic viscosity of the material. Furthermore, the fluid is assumed to be incompressible and the mass and momentum conservation equations are given as follows:

$$\underline{\nabla}\cdot\underline{v} = 0 \tag{2}$$

$$\rho\frac{D\underline{v}}{Dt} = -\underline{\nabla}p + \underline{\nabla}\cdot\underline{\underline{S}} + \rho\underline{g} \tag{3}$$

where $\underline{v}$ is the local velocity vector, ρ is density, p is pressure and g denotes gravity. The viscous dissipation and non-Newtonian effects are reflected in the definition of the extra stress tensor $\underline{\underline{S}}$, which depends on bulk viscosity following $\underline{\underline{S}} = 2\eta(D_{II})\underline{\underline{D}}$.

2.2. The porous medium influence

In various engineering fields, flow of complex fluids through periodic Porous Medium (PM) was thoroughly studied and led to the development of some sophisticated models [28,29]. To evaluate the influence of periodic PM on the flow, most authors use macroscopic averaging methods, where Eqs. (1) and (3) are modified to account for the presence of the porous matrix as a continuous medium [30]. The periodic PM is usually mathematically pictured as an equivalent bundle of capillaries with an average hydraulic radius being defined in terms of PM macroscopic parameters and/or properties such as porosity and permeability [28]. This results in the implementation of a modified version of the Darcy's Law for non Newtonian fluids in periodic PM.

From a computational point of view, the influence of the PM on the flow is modeled by the addition of a momentum source term to the standard momentum flow equations (right side of Eq. (3)). Since flow in industrial casting of concrete is mostly laminar, the inertial loss term can be neglected and the source term is only composed of a

viscous loss term. The model reduces to Darcy's Law and the added momentum source term S_i in the direction i is:

$$S_i = -\frac{\eta_{app}}{k_i} v_i \tag{4}$$

where η_{app} is the local apparent viscosity, k_i is the permeability coefficient in the direction i and v_i is Darcy's velocity in the direction i. For Newtonian materials, apparent viscosity is the Newtonian viscosity of the material. However, for Bingham materials, apparent viscosity depends on the local strain rate in the flowing material.

As the local strain rate within the PM is unknown and is a complex function of the geometry and configuration of the steel bars, it is necessary to define a so-called "apparent" shear rate $\dot{\gamma}_{app}$ within the medium as:

$$\dot{\gamma}_{app} = \frac{\alpha \cdot v_i}{\sqrt{k_i \cdot \phi}} \tag{5}$$

where ϕ is the PM porosity [31]. The coefficient α is the so-called "shift factor" (also called "shape factor"). The value of α is either measured through experiments [32] but also computed using pore-scale modeling approaches [29]. In [28] an overview of theoretical and empirical models, which relate Darcy's velocity of the material propagating and equivalent shear rate within the media, is given for flows of polymers in porous media. No matter the chosen approach, all authors show that the average apparent shear rate in the PM $\dot{\gamma}_{app}$ is a linear function of $v_i / \sqrt{k_i \phi}$, where v_i and k_i are Darcy's velocity and permeability in for the direction i. The shift factor α is equal to $4/\sqrt{8} \cong 1.41$ for bundle of capillaries of uniform diameter [28] whereas experimentally measured values of α lie in the range of 1.5 to 2.5 for packed glass beads and in the range of 4 to 7 for sand grains. In [29,33], the authors adjusted α to fit the analytical solutions obtained using 3D pore scale models with experimental and numerical data. Reported values for α lie in the range 1 to 5.2, and vary with different porous media and fluid systems.

Pearson and Tardy [30] reviewed the different mathematical approaches used to describe non-Newtonian flow in porous media. They concluded that, although α is, in most studies, considered as constant, it is a weak function of both bulk rheology and pore structure and that there is currently no theory able to predict its value reliably. We will, in the present study, calibrate α for a large range of materials representative of fluid concrete casting and for parallel cylinders configurations representative of reinforcement steel bars.

By introducing apparent shear rate into constitutive Eq. (1), the local apparent viscosity in PM writes:

$$\eta_{app}(\dot{\gamma}_{app}) = \frac{\tau_0}{\dot{\gamma}_{app}} + \eta_{pl} = \frac{\tau_0 \cdot \sqrt{k_i \cdot \phi}}{\alpha v_i} + \eta_{pl} \tag{6}$$

The source term in the momentum equation becomes:

$$S_i = -\frac{1}{k_i}\left(\frac{\tau_0 \cdot \sqrt{k_i \cdot \phi}}{\alpha} + \eta_{pl} v_i\right) \tag{7}$$

2.3. Validity of the proposed approach and Bingham number

Although it seems natural, as a first approximation, to write that the local apparent shear rate in PM is proportional to the macroscopic Darcy velocity, this simplification shall prove wrong, as discussed further, in the case of high Bingham numbers.

The Bingham dimensionless number expresses the relative contribution of yield stress and plastic viscosity. In the specific configuration studied in this paper, it writes:

$$B_n = \frac{\tau_0}{\eta_{pl} \dot{\gamma}_{app}} \tag{8}$$

High Bingham numbers are associated to flow regimes in which the contribution of yield stress exceeds and dominates the contribution of plastic viscosity. In these cases, some non-neglectable unsheared zones may exist between the bars. The local apparent shear rate may therefore not be proportional to the macroscopic flowing velocity anymore (see the discussion about α above). We will however in the following show that Eq. (5) holds for the range of Bingham numbers of interest for concrete casting predictions in construction.

3. Analytical and numerical studies of porous medium parameters

In order to model the reinforced zone as a PM, one needs to obtain the values of porosity, permeability and shift factor. Although access to porosity is obvious, permeability and shift factor are unknown. They have to be computed *a priori*. In this section, we compute permeability and the value of the shift factor in the range of interest for concrete casting prediction.

3.1. Permeability computation

The intrinsic permeability of any PM only depends on its geometry and topology. It can be directly numerically computed or experimentally measured by a single steady-state measurement on a sample of given geometry crossed by a Newtonian fluid. The permeability k can be obtained from the Darcy's Law as:

$$k = \frac{\eta_0}{v}\frac{\Delta p}{\Delta L} \tag{9}$$

where η_0 is viscosity of the Newtonian fluid and v is the Darcy velocity. ΔL is the length of the PM and ΔP is the pressure drop (either numerically computed or experimentally measured) between the inflow and outflow boundaries of the PM.

In this paper, we do not carry out any experimental measurements of permeability. We however compute the permeability of the simple geometries shown in Fig. 2. These geometries consist in a rectangular array filled with vertical cylinders. A Newtonian fluid is injected with a constant inlet velocity. The permeability is then calculated from the pressure drop predicted by the CFD software using Eq. (9).

The obtained numerical results are compared in Fig. 3 with the analytical solution for the lower and upper bounds of permeability of parallel cylinders from [34] and prove to be in good agreement.

These lower and upper bounds for permeability of a periodic configuration of parallel cylinders are respectively given by:

$$K_{\substack{lower\\bound}} = -R\left(LN(\rho) + (1-\rho)^2/(1+\rho)^2\right)/4 \tag{10}$$

$$K_{\substack{upper\\bound}} = -R\left(LN(\rho) + \left(1-\rho^4\right)/2\left(1+\rho^4\right)\right)/4 \tag{11}$$

where R is half the distance between the centers of the cylinders and ρ is the ratio between the radius of the cylinders and R.

It is interesting to note that the PM analogy works perfectly fine in the case of a Newtonian fluid. No matter the geometry, the Newtonian viscosity or the inlet velocity, as long as the flow stays laminar, pressure drop and flow-rate are linearly related showing that, as expected in the case of simple Newtonian fluids, the reinforcement bars can be treated as a porous medium. The calculated permeability

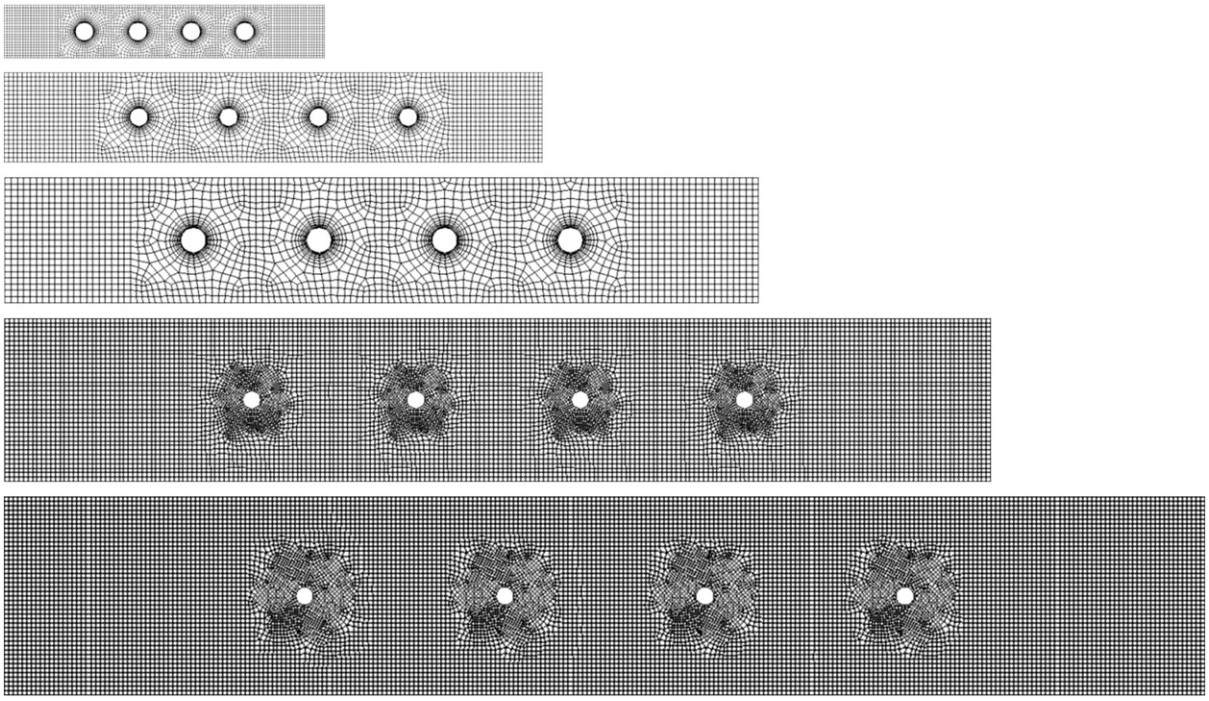

Fig. 2. Geometries used for the intrinsic permeability computation with a Newtonian fluid.

will be used further as an input parameter in the case of yield stress fluids propagating in identical PM.

3.2. Computation of the shift factor value

As discussed above, local apparent shear rate within a non-Newtonian fluid propagating through PM can be computed from the value of the macroscopic Darcy velocity of the fluid, the porosity, the permeability and the so-called shift factor α.

In order to compute the values of α and to examine its dependency on Bingham number, in this section, we conduct numerical case studies in various configurations (*i.e.* for a large range of Bingham numbers). The results of the simulations are shown in Fig. 4. Inlet velocity, distance between the bars and material properties are varied. The macroscopic apparent shear rate in the PM (to be distinguished from the local apparent shear rate defined in Eq. (5)) is calculated from the computed pressure drop in the porous medium.

$$\dot{\gamma}_{app}^{MACRO} = \frac{\tau_0}{\frac{k_i}{v_i}\frac{\Delta p}{\Delta L} - \eta_{pl}} \tag{12}$$

We then calculate the value of α so that the local apparent shear rate calculated from Eq. (5) equals the macroscopic apparent shear rate calculated from Eq. (12) on a range of Bingham numbers from 0.001 to 1000. On the studied range, it can be noted that α does only weakly depend on Bingham number as it varies between 1 for the lowest Bingham numbers and 1.5 for the highest ones.

In industrial practice, yield stress of fluid concretes, which this work could be applied to, is of the order of several hundreds of Pa. Their plastic viscosity is of the order of a couple hundreds of Pa. As a consequence, the above values for α are adequate as long as local apparent shear rate stays lower than a few hundreds of s^{-1} and higher than few hundredths of s^{-1}. These limit values are respectively well above and below the range of shear rates that are often considered during industrial casting (*i.e.* between 1 and 10 s^{-1} [15]). However, the lower boundary of this shear rate range prevents from the full prediction of flow stoppage during which shear rate slowly tends towards zero (Bingham number becoming infinite). It can be noted

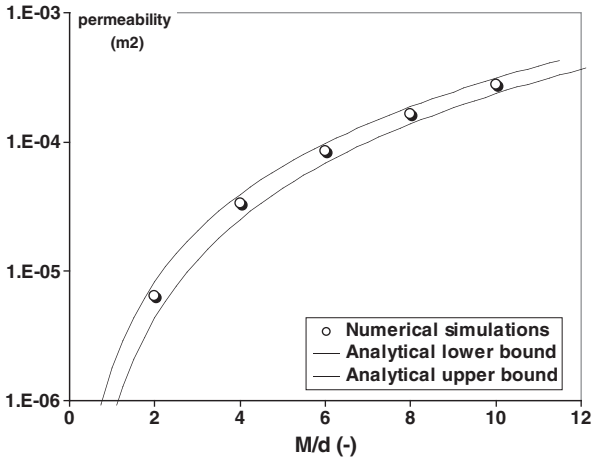

Fig. 3. Intrinsic permeability from numerical simulations of the flow of a Newtonian fluid as a function of the ratio between the distance between the bars and the diameter of bars. The bars diameter is 3 mm and they are located on a square lattice.

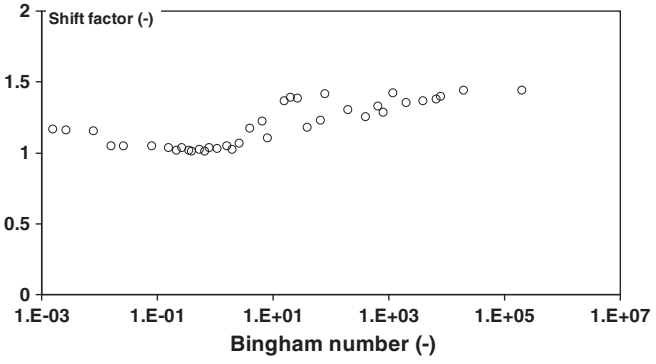

Fig. 4. Shift factor alpha as a function of the Bingham number.

that, in most practical cases, first order data are the ones dealing specifically with what happens when flow stops. These are the situations of interest when one wants to predict whether a given concrete will fill a given formwork or stop flowing before the mold is filled, leaving voids in the final structure. We will therefore in the following mainly focus on the shape of the concrete in the mold when flow stops. In order to ensure that the numerical tool presented in this paper is able to predict flow stoppage with the highest accuracy, we will in the following use $\alpha = 1.5$.

4. Model fluids and experimental results

4.1. Model materials

From a rheological point of view, fresh cementitious materials are thixotropic yield stress fluids. This means that these suspensions flow when the applied stress is higher than a critical value called the yield stress and that this yield stress strongly depends on the flow history of the material [8–16,35–38]. Moreover, these cementitious materials are submitted to a non-reversible chemical evolution (*i.e.* the hydration process), which strongly affects the rheological behavior on longer times of observation [39]. All these phenomena are of interest for the researcher trying to understand their physical origin and the practitioner trying to ensure that the casting process of these cementitious materials will allow for the proper filling of a given formwork. However, these phenomena being all mixed together in one material prevent most of the time both the researcher and the practitioner from being able to understand or predict anything. That is why being able to study model materials which display similar behavior as cementitious materials but with a lower degree of complexity are of very high interest.

We focus in this paper only on one aspect of the flow: the yield stress behavior. Nevertheless, in nature or industry, most yield stress fluids are also thixotropic. Two materials, which display a pure yield stress behavior, can however be found in literature: water/oil emulsion and carbopol suspension [40]. As the preparation of emulsion is highly time consuming as soon as volumes higher than a few liters are needed, we choose here to focus on carbopol. The polymer used in this work is Carbopol Ultrez (manufacturer Noveon) a transparent material that disperses faster than other conventional grades. Carbopol is used here at a volume fraction of 0.3%. As rheology of polymer solution is very sensitive to the chemical composition of solvent [41], in order to achieve a better reproducibility of the results, distilled water is chosen as the solvent. The manufacture of a suspension of Carbopol is divided in two stages: dispersion of the powder and neutralization of the solution [17].

The dehydrated Carbopol powder is slowly added to distilled water through a fine metal mesh using a variable speed mixer. The solution is then neutralized by a sodium hydroxide solution at 18%. A mixing period of 6 h follows this neutralization phase. Finally, the products are conserved at 25 °C during 2 days. The prepared carbopol suspension can then be diluted in distilled water in order to produce mixtures with yield stresses between 15 and 125 Pa. Before use, air bubbles are removed by a slow manual shearing.

The Carbopol suspension used in this study present neither thixotropic characteristic nor irreversible evolution [42]. This is shown by the superposition of the curves of increasing and decreasing rotating shear rate ramps in Fig. 5(left) and by the plastic plateau in Fig. 5(right). These curves are obtained using a HAAKE ViscoTester VT550 equipped with coaxial cylinders, the inner cylinder of diameter 18.9 mm being in rotation whereas the outer cylinder of diameter 20.5 mm remains fixed. Both cylinders surfaces are covered with sand paper in order to avoid wall slip. The modified gap width is identified using some reference Newtonian oil. In the following, we fit the behavior of all carbopol suspensions with a Bingham model.

4.2. Model formwork

The experimental setup used in this study is shown in Fig. 6 [17]. The setup consists of a $20 \times 20 \times 60$ cm container made of transparent Plexiglas, enabling observation of the flow front of the poured fluid. The adaptable modulus in the middle of the box, holds a variable number of vertical steel bars with diameter $d = 3$ mm. This system allows for easy modification of the number of bars and their configurations. Between 11 and 12 l of the carbopol suspension are slowly poured at one side of the form. The pouring speed was roughly 1 l/s to avoid any inertial effect [43]. We checked that final shape did not depend on pouring rate in this range and we kept the pouring height constant in each text. When flow stops, image analysis allows for the recording of the final shape of the material.

5. Comparison between CFD with steel bars, CFD with PM and experimental results

5.1. Simulation with no bars — boundary conditions

Since the interaction between carbopol suspensions and the solid Plexiglas wall of the model formwork are unknown, numerical studies on wall–fluid interaction are first conducted using the CFD software Fluent©. Among others, this software enables two different models for the fluid–wall interaction: wall slippage or no-slip condition. The experiments are performed by pouring the material into the model formwork without any steel bars and by recording the shape of the

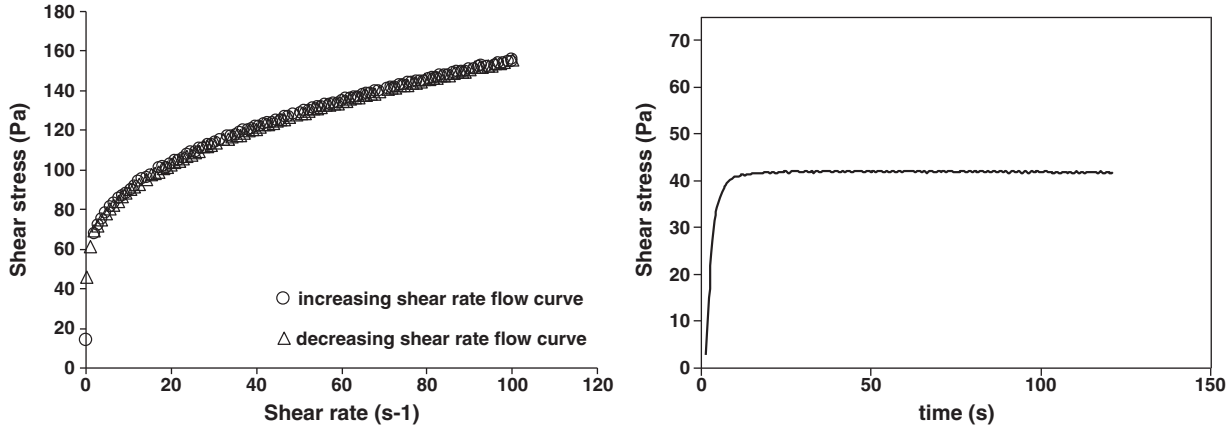

Fig. 5. Rheological behavior of the carbopol suspension used in this paper. (left) shear stress as a function of shear rate for increasing or decreasing shear rates (right) Yield stress measurement at a constant shear rate of 0.08 s^{-1} [42].

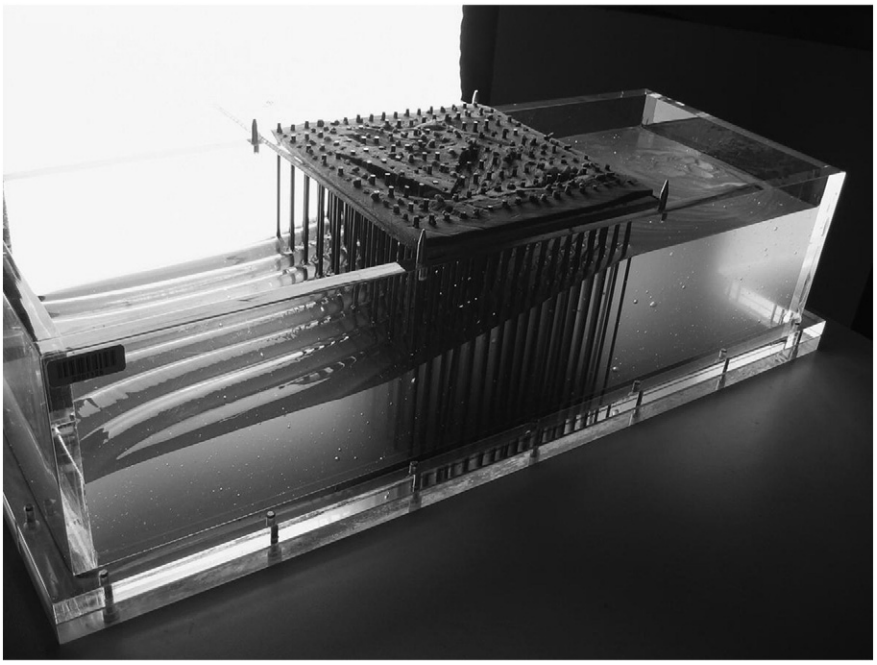

Fig. 6. Reduced model formwork casting.

free surface when flow stops. The carbopol suspension used in this section has the following properties: density $\rho = 990$ kg/m^3, plastic viscosity $\eta_{pl} = 1$ Pa·s, yield stress $\tau_0 = 20$ Pa.

The experiments are simulated using the two above boundary conditions at the lateral walls of the channel. The numerical set up is shown in Fig. 7. The material is numerically poured in the formwork using a pouring funnel. Fig. 8 shows the comparison of the experimentally obtained values with numerical studies. It can be observed that the best agreement is obtained when the no-slip condition is used on the bottom and the lateral walls of the formwork. This boundary condition is used in the rest of this paper.

5.2. Numerical simulation with steel bars and with PM

Numerical simulations of casting of carbopol suspensions in the model formwork with various steel bars configuration are carried out here using the software FLUENT©. The comparison between the predicted final shape and experimental measurements is plotted in Fig. 9. As already described in [1], CFD is able to predict the free surface flow of a yield stress fluid in a complex formwork.

In order to demonstrate applicability of the approach proposed in this paper on the reinforced sections, the same experiment is simulated using PM model. The PM model is implemented in FLUENT© as a User Defined Function (UDF) by adding a momentum source term in the porous medium (see Section 2.2). The permeability is obtained from numerical studies with Newtonian material (see Section 3.1), and the value of shift factor α used in the simulations is 1.5 (see Section 3.2).

Fig. 9 shows a comparison of the final shape of the material between experimental results, numerical simulation with the steel bars and numerical simulation for the corresponding PM case. Fig. 10 does not bring any additional scientific information but gives a visual representation of both experimental and numerical results obtained in the case of a 15 Pa carbopol suspension crossing a network of 3 mm steel bars located on a 22×22 mm grid. The total number of bars was 81.

The good correlation between experimental and numerical results shows that, although considering the steel bars network as a porous medium is a rough approximation, similar results are obtained for the final shape of the material after casting. This result validates the basic postulate of this study: when crossed by a yield stress fluid, the reinforcement network behaves as a porous medium and can be mathematically modeled as one.

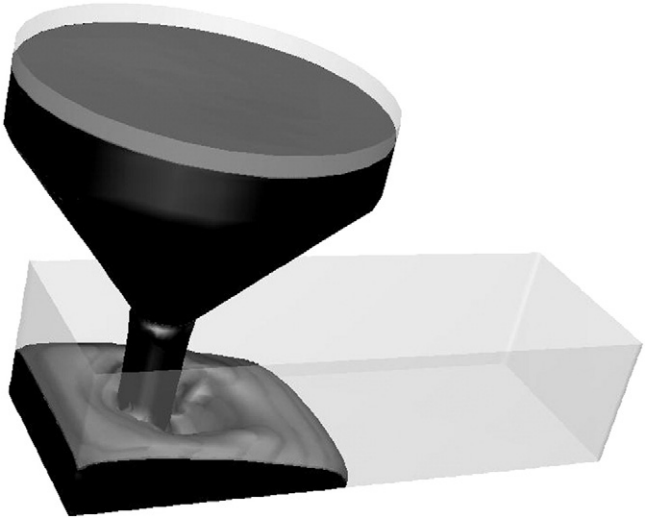

Fig. 7. Numerical set up for the calibration of the boundary conditions.

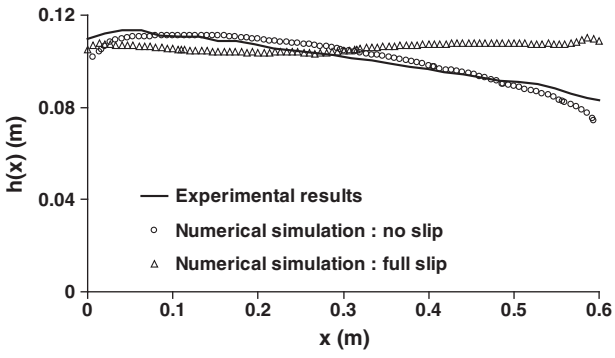

Fig. 8. Comparison of experimental shape with numerical simulations for the two types of boundary conditions.

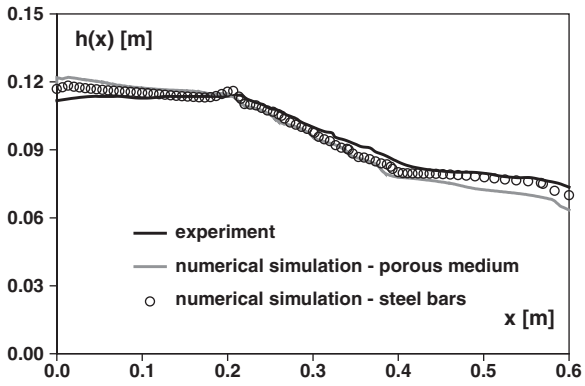

Fig. 9. Comparison between experimental measurements, numerical simulation with steel bars and numerical simulations with porous medium.

It can be noted that, in order to obtain the final shapes shown in Fig. 9, the following pre-processing times and computation times on the same computer were needed:

A) numerical simulation with steel bars:
Number of calculation cells: 170,000 cells (this mesh is, in theory, too coarse but had to be chosen in order to limit the computation time)
Pre-processing time: 2 h
Computation time: 10 h
Total time: 12 h

B) numerical simulation with porous medium
Number of calculation cells: 60,000 cells (this mesh is finer than actually needed)
Pre-processing time: 20 min
Computation time: 3.5 h
Total time: 4 h

Although only 70% reduction of total time is reached here, it can be noted that it would still be possible to reduce the number of calculation cells in the case of PM by a factor 3 decreasing therefore the total time to 1.5 h bringing it in the range of potential industrial applications.

Comparison between numerical simulations with steel bars or porous medium and experimental results are shown in Fig. 11 for a range of relative distances between the bars between 2.5 and 7 and various yield stresses between 15 and 40 Pa. The steel bars diameter is 3 mm. It can be noted that, in some cases, the material was not able to fully cross the porous medium both in the experiment and in numerical simulations. In order to gather all results in one graph, we choose here to plot the loss ratio defined as $\tau_0 \Delta x/\rho g \Delta h$ where τ_0 is the tested material yield stress, Δh is the thickness variation in the porous medium, Δx is equal to 0.2 m if the material crossed the porous medium or is equal to the propagating distance in the porous medium if it was not able to fully cross the porous medium.

It can be seen that, in the range of configurations tested here, the technique based on porous medium analogy is fully able to predict the shape of the cast material when flow stops. The average reduction in the total simulation time (both pre-processing and computation times) is 85%.

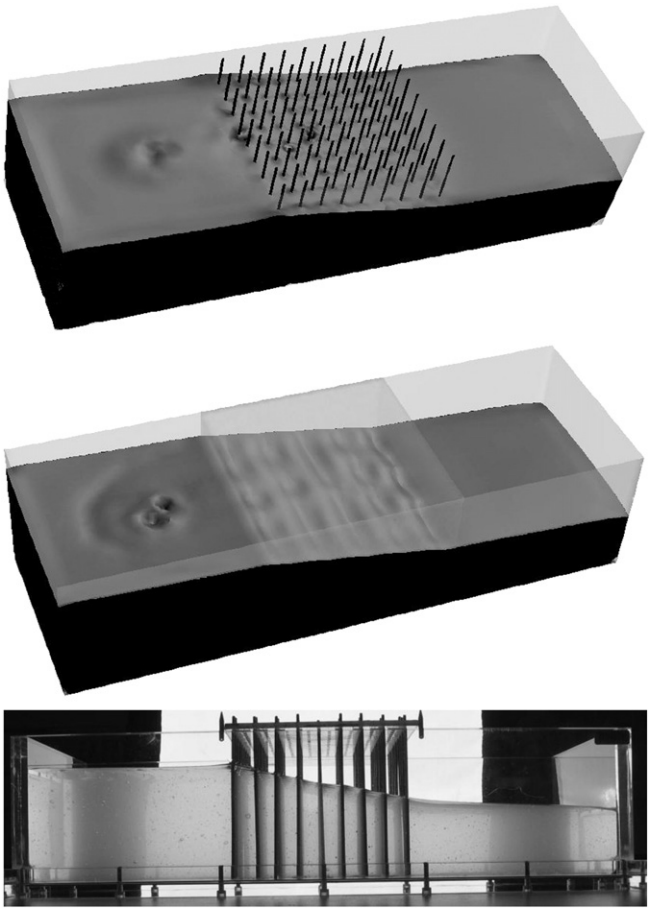

Fig. 10. Visual illustration of experimental and numerical results with steel bars or with porous medium.

6. Summary and conclusions

This paper presented a mathematical model for flow of concrete through reinforced sections modeled as a porous medium. It is based on computational fluid dynamics, coupling a single-phase flow model for concrete and a continuum macroscopic model for porous medium.

The numerical implementation of this concept was described. A methodology allowing for the computation of the equivalent permeability of the steel bars network was suggested. Finally, this numerical technique efficiency was evaluated through a comparison of numerical predictions with experimental results of model fluids castings in model formworks.

The comparison of experimental and numerical results showed that the proposed model is able to predict the final shape of the material. The time needed for the numerical simulations with PM

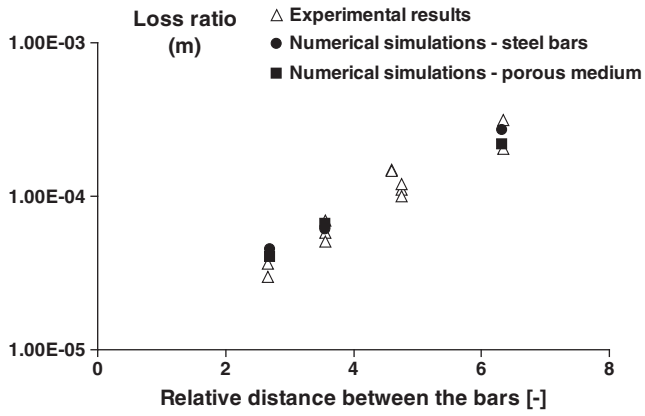

Fig. 11. Loss ratio $\frac{\tau_0 \Delta x}{\rho g \Delta h}$ as a function of the dimensionless distance between the bars (*i.e.* ratio between the distance between the bars and the diameter of the bars).

model was significantly shorter than for the simulations with reinforcement.

Future work will focus on studies with different reinforcement geometries, with the goal of defining a library of porous medium parameters for various classes of standard reinforcements.

References

[1] N. Roussel, Mr. Geiker, F. Dufour, Ln. Thrane, P. Szabo, Computational modeling of concrete flow: general overview, Cement and Concrete Research (2007), Cement and Concrete Research 37 (9) (2007) 1298–1307.

[2] V. Mechtcherine, S. Shyshko, Simulating the behaviour of fresh concrete using Distinct Element Method, in: G. De Schutter, V. Boel (Eds.), RILEM-Symposium on Self-Compacting Concrete SCC 2007, RILEM PRO, 54, 2007, pp. 467–472.

[3] M.A. Noor, T. Uomoto, Three-dimensional discrete element simulation of rheology tests of Self-Compacting Concrete, Proc. of the 1st Int. RILEM Symp. on SCC, 1999, pp. 35–46, Stockholm, Sweden.

[4] Ö. Petersson, H. Hakami, Simulation of SCC — laboratory experiments and numerical modeling of slump flow and L-box tests, Proc. of the 2nd Int. RILEM Symp. on SCC, 2001, pp. 79–88, Tokyo.

[5] Ö. Petersson, Simulation of self-compacting concrete — laboratory experiments and numerical modeling of testing methods, J-ring and L-box tests, Proc. of the 3rd Int. Symp. on SCC, August 2003, pp. 202–207, Reykjavik, Iceland.

[6] N. Martys, C.F. Ferraris, Simulation of SCC flow, Proc. 1st North American Conf. on the Design and Use of Self-Consolidating Concrete, Chicago, IL, 2002, pp. 27–30.

[7] H. Kuch, J.H. Schwabe, Achtagung Baumaschinentechnik 2003: Ausblick auf den Markt für Betonwaren und Betonfertigteile: Entwicklungstendenzen und -potenziale bei Fertigungsmaschinen zur Herstellung von Betonwaren und Betonfertigteilen, Betonwerk und Fertigteil-Technik 69 (6) (2003) 6–14, (in German).

[8] G.H. Tatersall, P.G.F. Banfill, The Rheology of Fresh Concrete, Pitman, London, 1983.

[9] C. Hu, F. de Larrard, The rheology of fresh high performance concrete, Cement and Concrete Research 26 (1996) 283–294.

[10] N. Roussel, Rheology of fresh concrete: from measurements to predictions of casting processes, Materials and Structures 40 (10) (2007) 1001–1012.

[11] N. Roussel, Correlation between yield stress and slump: comparison between numerical simulations and concrete rheometers results, RILEM Materials and Structures 39 (4) (2006) 501–509.

[12] D. Feys, R. Verhoeven, G. De Schutter, Fresh self compacting concrete, a shear thickening material, Cement and Concrete Research 38 (7) (July 2008) 920–929.

[13] Wallevik, J.E., Rheology of particle suspensions; fresh concrete, mortar and cement paste with various types of lignosulphonates. Ph.D. Thesis, Department of Structural Engineering, Norwegian University of Science and Technology 2003.

[14] N. Roussel, Steady and transient flow behaviour of fresh cement pastes, Cement and Concrete Research 35 (2005) 1656–1664.

[15] N. Roussel, A thixotropy model for fresh fluid concretes: theory, validation and applications, Cement and Concrete Research 36 (10) (2006) 1797–1806.

[16] N. Roussel, A. Lemaître, R.J. Flatt, P. Coussot, Steady state flow of cement suspensions: a micromechanical state of the art, Cement and Concrete Research 40 (2010) 77–84.

[17] Nguyen, T.L.H. (2007) « Outils pour la modélisation de la mise en œuvre des bétons », Doctoral thesis, Laboratoire central des Ponts et chaussées, ENPC p. 122 (in French).

[18] N. Roussel, « Ecoulement et mise en œuvre des bétons », OA 59, 2008, LCPC, ISSN 1161–028X (in French).

[19] K. Vasilic, B. Meng, H.C. Kühne, N. Roussel, Computational modelling of SCC flow: reinforcement network modelled as porous medium, The Rilem International Symposium on Rheology of Cement Suspensions, Reykjavik, August 19–21 2009.

[20] G.Y. Onoda, E. Liniger, Random loose packings of uniform spheres and the dilatancy onset, Physical Review Letter 64 (1990) 2727–2730.

[21] H. Okamura, O. Masahiro, Self compacting concrete, Journal of Advanced Concrete Technology 1 (1) (2003) 5–15.

[22] J. Yammine, M. Chaouche, M. Guerinet, M. Moranville, N. Roussel, From ordinary rheology concrete to self compacting concrete: a transition between frictional and hydrodynamic interactions, Cement and Concrete Research 38 (2008) 890–896.

[23] P. Coussot, Rheometry of Pastes, Suspensions and Granular Materials, John Wiley & Sons, New York, 2005.

[24] N. Roussel, T.L.H. Nguyen, O. Yazoghli, P. Coussot, Passing ability of fresh concrete: a probabilistic approach, Cement and Concrete Research 39 (2009) 227–232.

[25] N. Roussel, T.L.H. Nguyen, P. Coussot, General probabilistic approach of filtration process, Physical Review Letter 98 (11) (2007) 114502.

[26] C.T. Tam, A.M.M. Shein, K.C.G. Ong, C.Y. Chay, Modified J-ring approach for assessing passing ability of SCC, proceedings of SCC 2005, Hanley Wood, 2005.

[27] I.Y.T. Ng, H.H.C. Wong, A.K.H. Kwan, Passing ability and segregation stability of self-consolidating concrete with different aggregate proportions, Magazine of Concrete Research 58 (6) (2006) 447–457.

[28] K.S. Sorbie, P.J. Clifford, E.R.W. Jones, The rheology of pseudoplastic fluids in porous media using network modeling, Journal of Colloid and Interface Science 130 (1989) 508.

[29] X. Lopez, P.H. Valvatne, M. Blunt, Predictive network modeling of single-phase non-Newtonian flow in porous media, Journal of Colloid and Interface Science 264 (1) (2003) 256–265.

[30] J.R.A. Pearson, P.M.J. Tardy, Models for flow of non-Newtonian and complex fluids through porous media, Journal of Non Newtonian Fluid Mechanics 102 (2) (2002) 447–473.

[31] C.L. Perrin, P.M.J. Tardy, K.S. Sorbie, J.P. Crawshaw, Experimental and modeling study of Newtonian and non-Newtonian fluid flow in pore network micromodels, Journal of Colloid and Interface Science 295 (2006) 542–550.

[32] W.J. Canella, C. Huh, R.S. Seright, SPE 18089, Proceedings of SPE, 63 rd Ann. Tech. Conf. and Exhibition of SPE, Houston, TX, USA, 1988.

[33] M. Valvatne, X. Piri, M.J. Lopez, Blunt, Predictive pore-scale modeling of single and multiphase flow, Transport in Porous Media 58 (1–2) (2005) 23–41.

[34] C. Boutin, Study of permeability by periodic and self consistent homogenisation, European Journal of Mechanics 19 (2000) 603–632.

[35] P. Billberg, development of SCC static yield stress at rest and its effect on the lateral form pressure, in: S.P. Shah (Ed.), Proceedings of the Second North American Conference on the Design and use of Self-Consolidating Concrete and the Fourth International RILEM Symposium on Self-Compacting Concrete, October 30–November 3 2005, Chicago, USA.

[36] Y. Otsubo, S. Miyai, K. Umeya, Time-dependant flow of cement pastes, Cement and Concrete Research 10 (1980) 631–638.

[37] P.F.G. Banfill, D.C. Saunders, On the viscosimetric examination of cement pastes, Cement and Concrete Research 11 (1981) 363–370.

[38] J. Assaad, K. Khayat, H. Mesbah, Assessment of thixotropy of flowable and self-consolidating concrete, ACI Materials Journal 100 (2) (2003) 99–107.

[39] S. Jarny, N. Roussel, S. Rodts, F. Bertrand, R. Le Roy, P. Coussot, Rheological behavior of cement pastes from MRI velocimetry, Cement and Concrete Research 35 (2005) 1873–1881.

[40] F. Mahaut, X. Chateau, P. Coussot, G. Ovarlez, Yield stress and elastic modulus of suspensions of non-colloidal particles in yield stress fluids, Journal of Rheology 52 (1) (2008) 287.

[41] Y.I. Cho, J.P. Hartnett, Non-Newtonian fluids in circular pipe flow, Advances in Heat Transfer 15 (1982) 59–141.

[42] B.W. Barry, M.C. Meyer, The rheological properties of carbopol gels, International Journal of Pharmaceutics 2 (1979) 27–40.

[43] N. Roussel, Correlation between yield stress and slump: comparison between numerical simulations and concrete rheometers results, Materials and Structures 39 (4) (2006) 501–509.